Optical induction of synaptic plasticity using a light-sensitive channel

Yan-Ping Zhang & Thomas G Oertner

We have combined millisecond activation of channelrhodopsin-2 (ChR2), a light-gated ion channel, with two-photon calcium imaging to investigate active synaptic contacts in rat hippocampal slice cultures. Calcium influx was larger during light-induced action potentials than during action potentials induced by somatic current injection, leading to highly reproducible synaptic transmission. Pairing of light stimulation with postsynaptic depolarization induced long-term potentiation, making this technique ideal for genetic and pharmacological dissection of synaptic plasticity.

Long-term potentiation, a form of synaptic plasticity, is a primary experimental model for the study of cellular and molecular mechanisms underlying learning and memory. Several reports have suggested that there might be considerable heterogeneity in the expression of plasticity at individual synapses[1–3], but it has been difficult to measure both functional and morphological parameters of synapses at the same time[4–6]. Laser uncaging of glutamate has recently been used to study synaptic plasticity at identified spines[7,8]. Although it allows for excellent spatial resolution, this technique completely bypasses the presynaptic terminal and is therefore restricted to the investigation of postsynaptic mechanisms. Here we have developed a new approach that allows us to observe presynaptic varicosities and postsynaptic spines first, and then stimulate visually identified synaptic contacts precisely and uninvasively. We took advantage of a newly identified light-gated cation channel, ChR2, that can control neuronal activity with millisecond precision[9,10]. We modified a previously published construct[10] by tagging it with the red fluorescent protein tdimer2 (ref. 11; see **Supplementary Methods** online). Red labeling is advantageous for visualizing ChR2-positive neurons without activating the channel: under 546-nm illumination, ChR2 absorption is only ~4% of the maximum[9]. Using particle-mediated gene transfer, we obtained strong, stable expression of ChR2-tdimer2 in a small number of neurons in rat hippocampal slice cultures (**Supplementary Fig. 1** online).

First, we examined the light dependence of ChR2 currents in the presence of tetrodotoxin (TTX) to block action potentials. We recorded the membrane potential from ChR2-positive neurons using three standard filter sets for excitation: a green fluorescent protein (GFP) filter set (470/40, blue), a yellow fluorescent protein (YFP) filter set (500/20, blue) and a *Discosoma* red fluorescent protein (DsRed) filter set (546/11, green). Consistent with the published excitation spectrum of ChR2 (ref. 9), blue light was most efficient in activating the channel (**Fig. 1a**). In regular recording solution without TTX, the spike threshold was reached at 0.3 mW for blue light (5-ms light pulses) and at 7 mW for green light (DsRed filter set). Thus, we had a large safety margin to inspect the ChR2-tdimer2–transfected slice cultures in epifluorescence mode without triggering any spikes. Using the DsRed filter set, we could select cultures with a favorable expression pattern and target ChR2-postive cells for patch-clamp recordings.

As a standard stimulus, we used 5-ms pulses of blue light, which reliably triggered action potentials up to 10 Hz. At higher frequencies, action potentials became unreliable owing to permanent depolarization of the cell (**Supplementary Fig. 1**). We were interested in potential differences between light-evoked action potentials (AP_L) and action potentials evoked by brief somatic current injection (AP_C). Recording the somatic membrane potential during AP_L revealed a long-lasting depolarization after the action potential (**Fig. 1b**), suggesting that the ChR2 conductance outlasted and counteracted the repolarizing K^+ current. We investigated the time course of ChR2 currents in voltage-clamp recordings, and measured a decay time constant (τ_{decay}) of 32 ms in K^+-based intracellular solution (**Fig. 1c**). In Cs^+-based intracellular solution, which provides better space clamping of the cell, τ_{decay} was 10 ± 3 ms, and restricting the illumination to the soma further shortened τ_{decay} to 5 ± 1 ms, very similar to the turning-off rate of ChR2-YFP measured in a tumor cell line (PC12 cells)[12]. Thus, the long-lasting depolarization after the action potential (**Fig. 1b**) is mostly due to the large capacitance of the cells used, pyramidal cells of hippocampal area CA1.

As ChR2 is known to be permeable to Ca^{2+} ions[9], we set out to compare AP_L and AP_C with respect to the peak calcium levels reached in the cell. ChR2-positive neurons were loaded with a mixture of Fluo-5F and Alexa 594 through a patch-clamp electrode and imaged using two-photon excitation at 810 nm. At the intensities we used for calcium imaging (<30 mW), we did not detect any direct activation of ChR2 by the imaging laser (**Supplementary Fig. 1**). Action potentials induced by blue light pulses (5 ms) triggered simultaneous fluorescence changes in basal dendrites and spines (**Fig. 1d**). To compare calcium transient amplitudes, we normalized the fluorescence change of Fluo-5F to the fluorescence intensity in the red channel ($\Delta G/R$)[13]. $\Delta G/R$ was significantly larger when the action potential was trigged by light (**Fig. 1e**; $P < 0.05$). To investigate the mechanism of the additional calcium influx, we applied the Na^+ channel blocker TTX (1 μM), which completely blocked AP_C and the subsequent calcium influx

Friedrich Miescher Institute, Novartis Research Foundation, Maulbeerstr. 66, WRO-1066.4.04, CH-4058 Basel, Switzerland. Correspondence should be addressed to T.G.O. (thomas.oertner@fmi.ch).

RECEIVED 23 JUNE; ACCEPTED 1 NOVEMBER; PUBLISHED ONLINE 31 DECEMBER 2006; DOI:10.1038/NMETH988

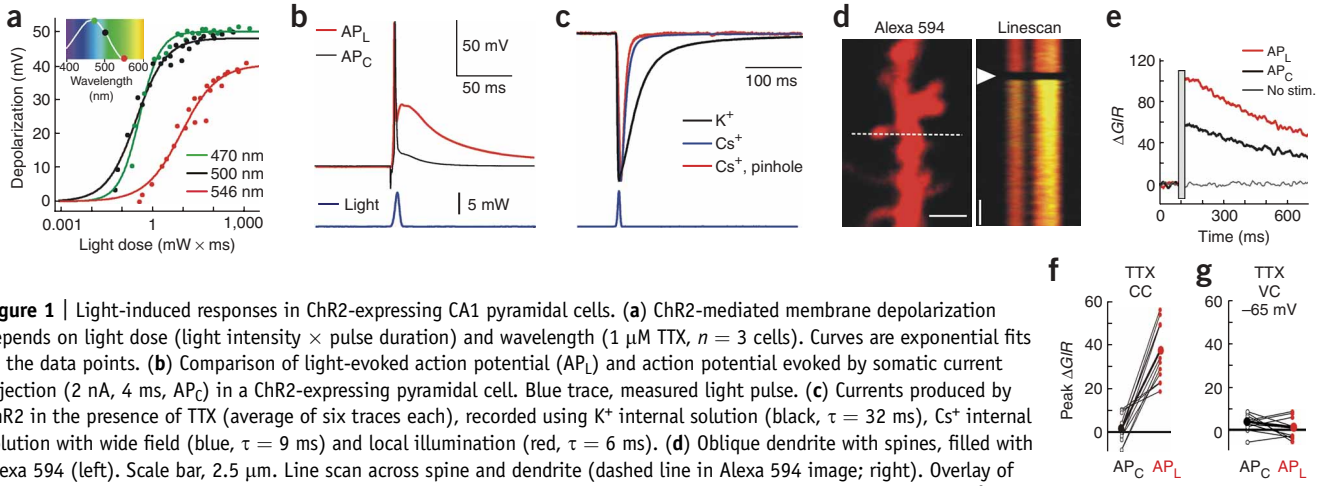

Figure 1 | Light-induced responses in ChR2-expressing CA1 pyramidal cells. (**a**) ChR2-mediated membrane depolarization depends on light dose (light intensity × pulse duration) and wavelength (1 μM TTX, $n = 3$ cells). Curves are exponential fits to the data points. (**b**) Comparison of light-evoked action potential (AP_L) and action potential evoked by somatic current injection (2 nA, 4 ms, AP_C) in a ChR2-expressing pyramidal cell. Blue trace, measured light pulse. (**c**) Currents produced by ChR2 in the presence of TTX (average of six traces each), recorded using K^+ internal solution (black, $\tau = 32$ ms), Cs^+ internal solution with wide field (blue, $\tau = 9$ ms) and local illumination (red, $\tau = 6$ ms). (**d**) Oblique dendrite with spines, filled with Alexa 594 (left). Scale bar, 2.5 μm. Line scan across spine and dendrite (dashed line in Alexa 594 image; right). Overlay of green (Fluo-5F) and red fluorescence (Alexa 594). Arrowhead indicates light-induced action potential. (**e**) Dendritic Ca^{2+} transients evoked by a single AP_L (red trace), single AP_C (black) and no stimulation (gray). Average of 21 dendrites, 4 cells. (**f**) Effect of TTX on peak dendritic calcium transients during AP_C and AP_L ($n = 12$, averaged over ten trials each; thick line, average of all experiments). (**g**) Peak Ca^{2+} transients measured in voltage clamp at –65 mV in the presence of TTX ($n = 10$, ten trials each; thick line, average).

(**Fig. 1f**). The light pulse, in contrast, still caused a calcium transient, which was similar in amplitude to the difference between the calcium transients during AP_C and AP_L. In case of direct calcium influx through ChR2 channels, preventing the cell depolarization should increase the calcium influx owing to the increased driving force on Ca^{2+} ions at more negative potentials. Light stimulation under voltage-clamp conditions (–65 mV), however, did not evoke any detectable calcium influx (**Fig. 1g**), although the rapid depolarizing current recorded at the soma indicated that the ChR2 channel was still functional (data not shown). We concluded that the additional calcium influx seen during light-induced action potentials was mainly due to activation of voltage-gated calcium channels during the after-depolarization following an AP_L (**Fig. 1b**), not to calcium influx through the pore of ChR2 itself.

Because of the high degree of connectivity in mature hippocampal slice cultures[3], it was straightforward to record light-induced excitatory postsynaptic currents ($EPSC_L$) in ChR2-negative CA1 neurons in cultures containing at least one ChR2-expressing neuron in area CA3. Moving the illuminated spot from CA3 to CA1 changed the latency of the $EPSC_L$ from ~7 ms to 0 ms (**Supplementary Fig. 2** online), indicating the generation of a local AP_L in the axon. For comparison, we performed intracellular recordings of connected pairs of a CA3 and a CA1 pyramidal cell. Paired recordings resulted in excitatory postsynaptic currents ($EPSC_P$) of rather uniform amplitude (23 ± 6 pA), whereas $EPSC_L$ often had larger amplitudes (54 ± 33 pA; **Supplementary Fig. 2**), probably owing to the stimulation of more than one connected axon. The coefficient of variation was significantly smaller in $EPSC_L$ ($CV_L = 0.24 \pm 0.09$, $CV_P = 0.48 \pm 0.20$, $P < 0.05$, Mann-Whitney U test), suggesting that there is an increased release probability, p_r, after an AP_L. The light-induced responses were well fit by a Monte Carlo simulation of glutamate release assuming quantal size $q = 15$ pA and $p_r = 0.8$ (**Supplementary Fig. 2**). Artificially depressing p_r by adding 2-chloroadenosine to the recording solution increased the variability of $EPSC_L$ to values similar to those for $EPSC_P$ (**Supplementary Fig. 2**). We conclude that AP_L increases the synaptic release probability, which is corroborated by the strong paired-pulse depression that we always observed with light stimulation.

The most direct way to measure release probabilities at individual synaptic contacts is spine calcium imaging. *N*-Methyl-D-aspartate (NMDA) receptors activated by presynaptic glutamate

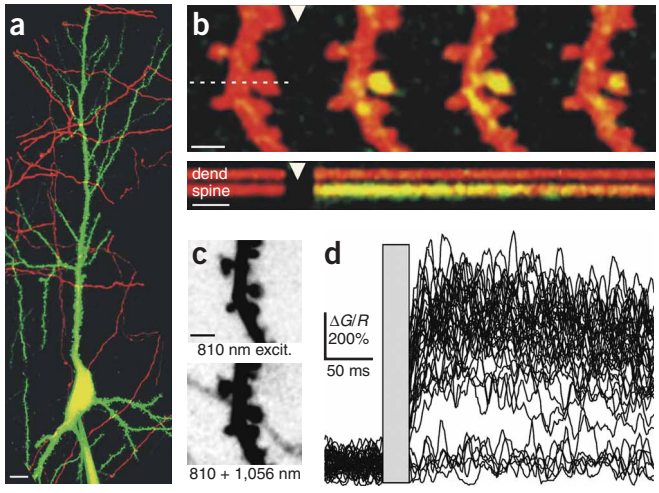

Figure 2 | Imaging postsynaptic calcium transients following light-induced action potentials in the presynaptic axon. (**a**) Single CA1 pyramidal cell filled with Fluo-5F and Alexa 594 in proximity to ChR2-expressing axons (red). Overlay of 810-nm excitation image (green) and 1,056-nm excitation image (red). Scale bar, 10 μm. (**b**) Top, overlay of green (Fluo-5F) and red fluorescence (Alexa 594). Ca^{2+} transient after light stimulation (arrowhead) is restricted to a single spine (yellow). White line indicates position of line scan. Scale bar, 2 μm. Bottom, line scan (single trial) across dendrite (dend) and spine head (spine). Scale bar, 50 ms. (**c**) Visualization of potential synaptic contacts by simultaneous imaging of ChR2-tdimer2–expressing axon (1,056-nm excitation) contacting Alexa 594–labeled spine (810 nm). Scale bar, 2 μm (**d**) Spine calcium transients and transmission failures evoked by 5-ms light pulses (42 consecutive trials).

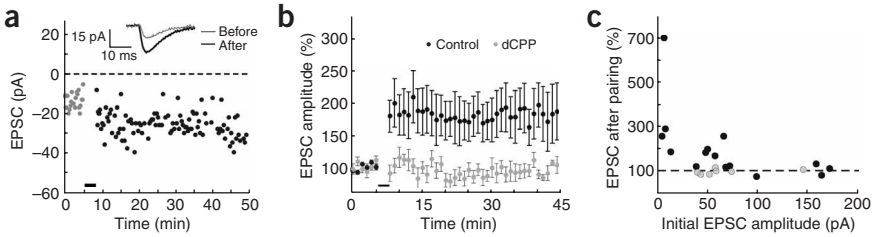

Figure 3 | Potentiation of light-induced synaptic responses. (**a**) Amplitude of light-induced synaptic responses plotted as a function of time. After 6 min of baseline recording, ten light-induced EPSCs were paired with brief postsynaptic depolarizations (voltage step to –15 mV for 100 ms) at 0.1 Hz, resulting in a stable increase in response amplitude to 187% of baseline. Horizontal bar indicates time of pairing. Inset, average EPSCs before and after pairing. (**b**) The pairing protocol led to stable long-term potentiation of 168% ± 29% (black markers, mean ± s.e.m., $n = 22$ cells). Blockade of NMDA receptors with dCPP prevented the potentiation of light-induced responses (gray markers, $n = 9$ cells). (**c**) Potentiation plotted as a function of initial EPSC amplitude. EPSCs were averaged in a 10-min time window, 20–30 min after pairing. Black, significant change ($P < 0.05$, Student's *t*-test, two-tailed); gray, change not significant.

release trigger calcium transients in dendritic spines, which can be readily detected by two-photon microscopy[14]. We identified potential points of contact between the dendrite of a dye-filled CA1 pyramidal cell and ChR2-positive axons (**Fig. 2**). Testing 33 potential contacts by two-photon calcium imaging, we found three functional synapses (**Fig. 2b**). At functional synapses, successes and failures of glutamate release could be clearly distinguished (**Fig. 2d**; 42 trials, 6 failures). Release probability was very high in all cases ($p_r = 0.89 \pm 0.09$, $n = 3$), in line with the low variability of $EPSC_L$ (**Supplementary Fig. 2**). Clearly, ChR2-expressing axonal terminals provide a highly reliable and precisely timed source of glutamate, and two-photon calcium imaging can be used to verify putative synaptic contacts without the need for electron microscopic reconstruction.

We were interested in whether the light stimulation technique could be used to induce long-term potentiation of synaptic connections in CA1. Our induction protocol consisted of $EPSC_L$ paired with brief postsynaptic depolarizations (100 ms to $V_m = –15$ mV) at 0.1 Hz. After ten pairings, $EPSC_L$ amplitudes increased significantly (**Fig. 3a**; $P < 0.05$). The increase was stable for the duration of the recording (up to 90 min). On average, the excitatory postsynaptic current was potentiated to 168% ± 29% (mean ± s.e.m., $n = 22$ cells) of the control amplitude (**Fig. 3b**). Potentiation was completely prevented in recording solution containing 10 μM dCPP, an NMDA receptor blocker, suggesting that the potentiation was NMDA receptor dependent (**Fig. 3b**). The magnitude of potentiation was inversely correlated with the amplitude of the excitatory postsynaptic current before potentiation: all connections with initial excitatory postsynaptic current amplitudes <40 pA, but only half of the connections between 40 and 170 pA, showed significant potentiation (**Fig. 3c**; $P < 0.05$). The inverse correlation might indicate that strong synaptic connections have already undergone potentiation during the culture period. Our results are virtually identical to those of published long-term potentiation experiments carried out on connected pairs of CA3-CA1 pyramidal cells using dual patch-clamp recordings[3], suggesting that the development of synaptic connections proceeds undisturbed in cells expressing ChR2.

Remote control of synaptic transmission by light combined with two-photon imaging provides a new avenue for investigating plasticity at the single-synapse level. As compared to stimulation by extracellular electrodes, light stimulation is very selective. This mitigates the typical problems with recurrent excitation in organotypic slice cultures and makes it unnecessary to reduce excitability by adenosine receptor agonists[15]. Compared to multiple patch-clamp recordings, light stimulation has a much higher throughput and allows contacts to be visualized with ease; however, in densely transfected cultures wide-field illumination may activate multiple axons. Light stimulation is not limited to excitatory synapses: in cultures with ChR2-positive interneurons, we frequently observed inhibitory postsynaptic responses (data not shown). The increased calcium influx during ChR2 activation reported here (**Fig. 1**) has important consequences, especially for the design of transgenic animals expressing ChR2; unfocused blue light not only will trigger spikes, but also might induce synaptic plasticity by providing (i) a high release probability at ChR2-positive axons and (ii) additional calcium influx at ChR2-positive dendrites and spines. In summary, ChR2 is a powerful tool to selectively activate neurons and to modify neuronal circuits by changing synaptic efficacy.

Note: Supplementary information is available on the Nature Methods website.

ACKNOWLEDGMENTS

We thank K. Deisseroth and G. Nagel for the ChR2-YFP construct, R.Y. Tsien and K. Svoboda for the generous gift of tdimer2 and the synapsin expression vector, D.G. Erni for excellent technical assistance, and T. Rose and A. Lüthi for critical discussions.

COMPETING INTERESTS STATEMENT

The authors declare that they have no competing financial interests.

Published online at http://www.nature.com/naturemethods/
Reprints and permissions information is available online at http://npg.nature.com/reprintsandpermissions/

1. Petersen, C.C., Malenka, R.C., Nicoll, R.A. & Hopfield, J.J. *Proc. Natl. Acad. Sci. USA* **95**, 4732–4737 (1998).
2. Isaac, J.T. *et al. Neuropharmacology* **37**, 1399–1410 (1998).
3. Debanne, D., Gahwiler, B.H. & Thompson, S.M. *J. Neurosci.* **19**, 10664–10671 (1999).
4. Koester, H.J. & Sakmann, B. *Proc. Natl. Acad. Sci. USA* **95**, 9596–9601 (1998).
5. Engert, F. & Bonhoeffer, T. *Nature* **399**, 66–70 (1999).
6. Holthoff, K., Tsay, D. & Yuste, R. *Neuron* **33**, 425–437 (2002).
7. Matsuzaki, M., Honkura, N., Ellis-Davies, G.C. & Kasai, H. *Nature* **429**, 761–766 (2004).
8. Bagal, A.A., Kao, J.P., Tang, C.M. & Thompson, S.M. *Proc. Natl. Acad. Sci. USA* **102**, 14434–14439 (2005).
9. Nagel, G. *et al. Proc. Natl. Acad. Sci. USA* **100**, 13940–13945 (2003).
10. Boyden, E.S., Zhang, F., Bamberg, E., Nagel, G. & Deisseroth, K. *Nat. Neurosci.* **8**, 1263–1268 (2005).
11. Campbell, R.E. *et al. Proc. Natl. Acad. Sci. USA* **99**, 7877–7882 (2002).
12. Ishizuka, T., Kakuda, M., Araki, R. & Yawo, H. *Neurosci. Res.* **54**, 85–94 (2006).
13. Yasuda, R. *et al. Sci. STKE* **2004**, 15 (2004).
14. Oertner, T.G., Sabatini, B.L., Nimchinsky, E.A. & Svoboda, K. *Nat. Neurosci.* **5**, 657–664 (2002).
15. Shi, S., Hayashi, Y., Esteban, J.A. & Malinow, R. *Cell* **105**, 331–343 (2001).

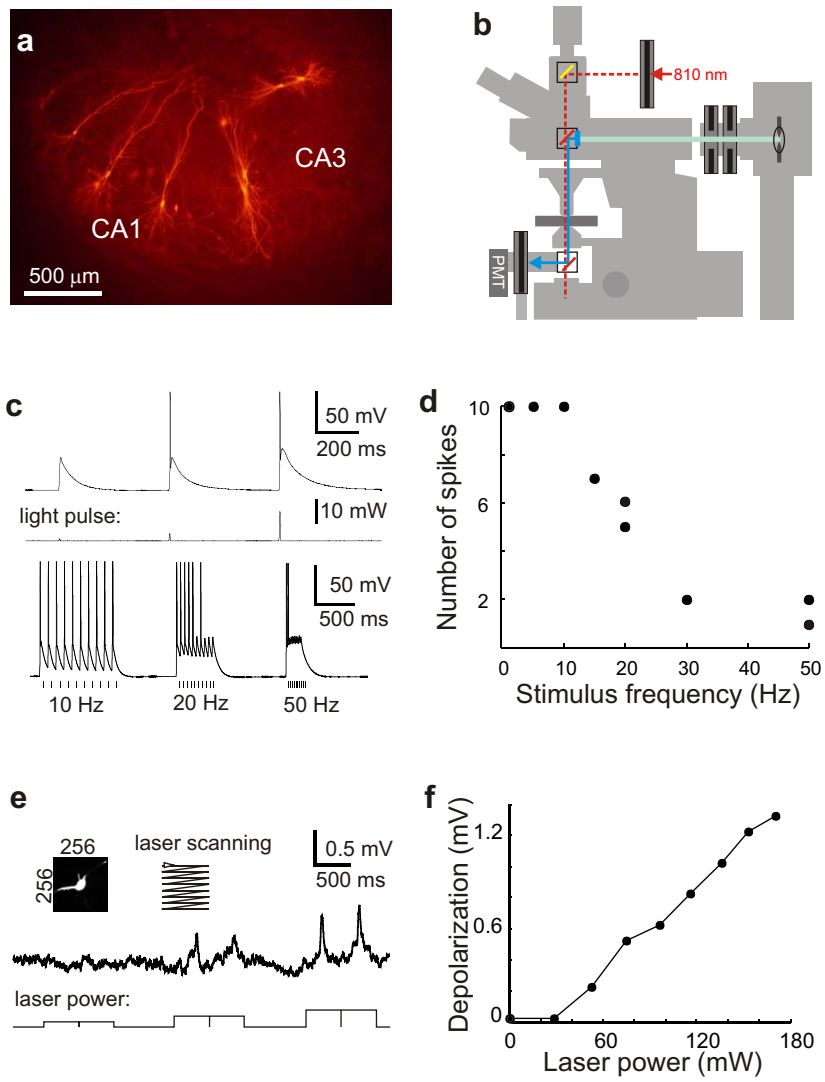

Supplementary Figure 1. Light stimulation using single-photon and two-photon excitation. (**a**) Hippocampal neurons expressing ChR2-tdimer2. (**b**) Schematic drawing of the shutter system used to combine light stimulation with two-photon imaging. (**c**) Top: Voltage trace showing subthreshold depolarization and action potential generation in a ChR2 expressing neuron evoked by 470 nm light pulses (5 ms) at different intensities (stimulus trace below). Bottom: Responses to repetitive stimulation by 5 ms light pulses at 10, 20, and 50 Hz. (**d**) In response to a burst of 10 light pulses, action potentials were reliably induced up to 10 Hz. At higher frequencies, cells became permanently depolarized and failed to spike reliably. (**e**) Voltage trace showing membrane depolarization of a ChR2 expressing cell in response to laser scanning across the soma at 810 nm (2 frame scans, 500 ms each) at 30, 80, and 140 mW average laser power. Only at high laser intensities, small depolarizations were detectable. (**f**) Membrane depolarization depends on laser power (810 nm). Typical intensities used for calcium imaging were < 30 mW.

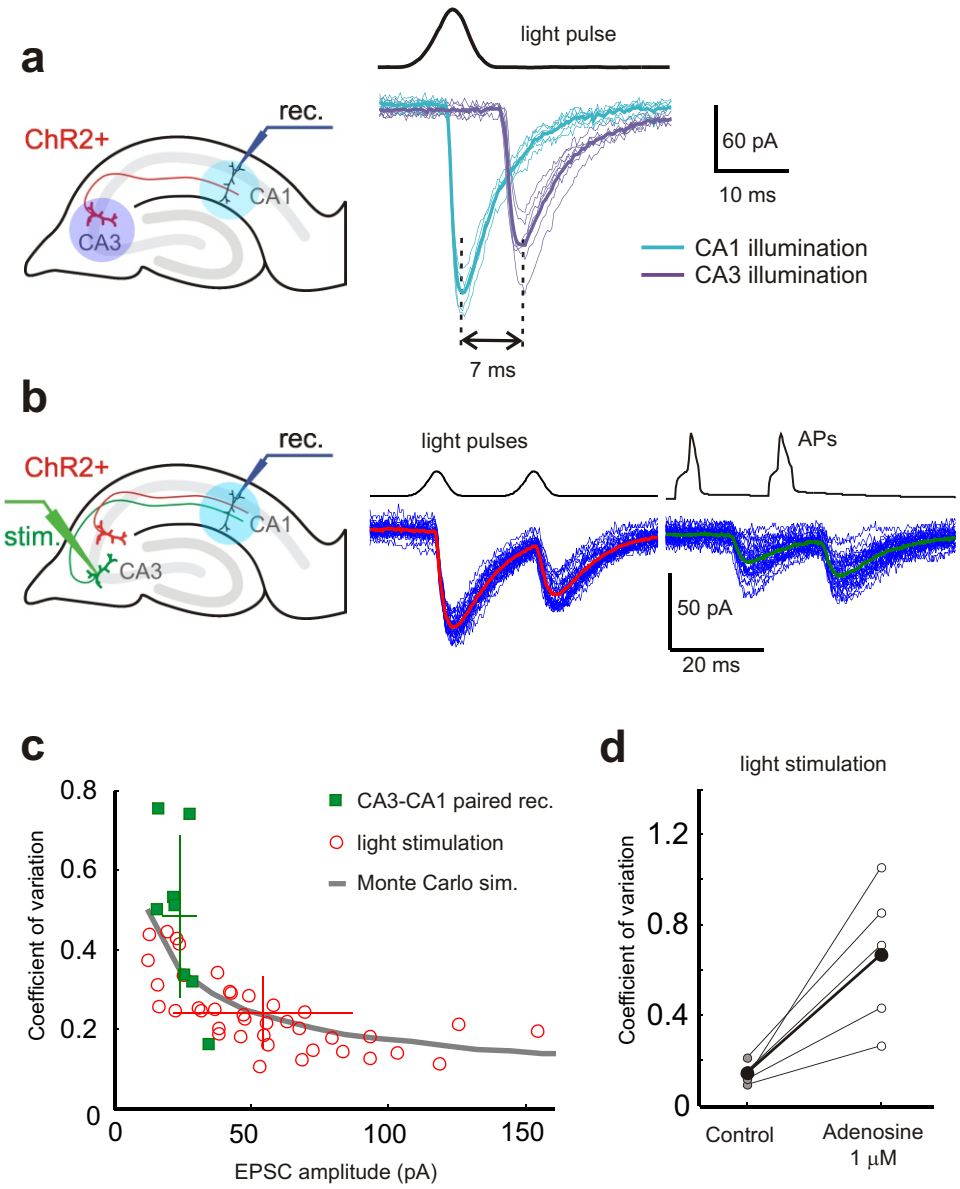

Supplementary Figure 2. Comparison of light-evoked synaptic responses and paired recordings. (**a**) Illuminating a ChR2-expressing cell in CA3 caused delayed EPSCs in a synaptically connected CA1 pyramidal cell (blue traces). Illuminating CA1 at the same intensity led to instantaneous EPSCs in the same postsynaptic CA1 pyramidal cell (green traces), indicating local action potential generation in the axon. (**b**) Simultaneous patch clamp recording of a connected pair of non-transfected CA3 and CA1 pyramidal cells in a slice culture containing also ChR2-expressing cells (red). EPSCs recorded in single CA1 cell in response to stimulation of presynaptic axons by a pair of light pulses (left, duration = 5 ms, ISI = 20 ms) and by a pair of APs in a single connected CA3 cell (right). Note small trial-to-trial variability, paired-pulse depression, and short latency of the light-evoked responses. (**c**) Summary of paired recording experiments (green squares, n = 8 pairs) and stimulation of presynaptic axons by light (red circles, n = 39 cells). Crosses indicate mean ± s.d. Gray line: Result of Monte-Carlo simulation with q =15 pA and p_r = 0.8. Note that many paired recordings have higher CV, indicating release probabilities < 0.8. (**d**) Variability of light-evoked synaptic response strongly increases after decreasing synaptic release probability by 1 μM 2-Chloroadenosine (n = 5 cells, thick line: average).

Supplementary Methods

Plasmid construction: The cDNA encoding ChR2-YFP, a gift from Karl Deisseroth, was subcloned into a neuron-specific expression vector (Synapsin-1 promoter vector[1]) via *Nhe*I and *Bam*HI restriction sites by PCR with primers:
5'-ATT*GCTAGC*CACCATGGATTATGGAGGCGCCCTG-3' and
5'-ATT*GGATCC*TTACTTGTACAGCTCGTCCATGCC-3'. The ChR2-tdimer2 construct was then generated by replacing the YFP gene with tdimer2(12) via *Not*I and *Sal*I restrictions sites using PCR with primers:
5'-ATT*GCGGCCGC*CATGGTGGCCTCCTCCGAGGACG-3' and
5'-ATT*GTCGAC*CTACAGGAACAGGTGGTGGCGG-3'. The constructs were verified by DNA sequencing, amplified and purified using MaxiPrep Kits (Qiagen).

Slice culture and transfection: Organotypic hippocampal slices were prepared from Wistar rat at postnatal day 5 as described[2], in accordance with the animal care and use guidelines of the Veterinary Department Basel-Stadt. After 7-10 days *in vitro*, cultures were biolistically transfected with the synapsin-ChR2-tdimer2 construct, using a Helios Gene Gun (BioRad). Light stimulation experiments were performed 2-3 weeks after transfection. No extra retinal was added to either culture medium or recording solution.

Electrophysiology: Hippocampal slice cultures were placed in the recording chamber of the microscope and superfused with artificial cerebrospinal fluid (ACSF) containing (in mM): 119 NaCl, 2.5 KCl, 4 $CaCl_2$, 4 $MgCl_2$, 26.2 $NaHCO_3$, 1 NaH_2PO_4, 11 glucose. The solution was gassed with 95% O_2, 5% CO_2, pH was adjusted to 7.2. Single and dual whole-cell recordings were performed using Axopatch 200B and MultiClamp 700B amplifiers (Axon Instruments). For current-clamp experiments, the recording pipettes (4.5 - 5.5 MΩ) were filled with intracellular solution containing (in mM): 140 K-$MeSO_4$, 10 HEPES, 4 $MgCl_2$, 4 Na_2-ATP, 0.4 Na_2-GTP, 10 Na_2-phosphocreatine, 3 ascorbate, 0. 03 Alexa Fluor 594 and 0.6 fluo-5F. Voltage-clamp experiments were compensated for series resistance and whole-cell capacitance, and K^+ was replaced by Cs^+. For imaging of postsynaptic calcium transients, cells were voltage-clamped at +40 mV. For LTP

experiments, EGTA (0.6 mM) was used instead of fluo-5F. Measurements are given as mean ± standard deviation, unless indicated otherwise.

Light stimulation and 2-photon imaging: The custom-build 2-photon imaging setup was based on an Olympus BX51WI microscope equipped with a LUMPlan W-IR2 60× 0.9 NA objective, controlled by a free software package[3] written in Matlab (The MathWorks). Emitted fluorescence was detected through an oil immersion condenser (1.4 NA, Olympus). A recording chamber with a 1 mm quartz glass bottom (wzw-optic AG) was used to minimize glass phosphorescence after the blue light pulse. We used two mechanical shutters (VS25, Uniblitz) in front of a 100W Hg arc lamp (Olympus) to deliver light pulses for ChR2 activation. Two shutters were needed to keep millisecond timing in spite of intense heat build-up by the arc lamp. Time course and intensity of the light pulse were measured below the condenser using a photomultiplier protected by neutral density filters. The shortest pulses we could produce were 5 ms full-width at half-maximum. To calibrate the intensity measurements for each wavelength, we measured the light intensity at the back aperture of the objective with a commercial power meter (LaserCheck, Coherent). Two PMTs below the condenser were used to detect red and green emission (R3896, Hamamatsu). During the light pulse, they were protected by an additional VS25 shutter (see Supplementary Fig. 1B). Two ultrafast IR lasers (ChameleonXR, Coherent; GLX-200, Time-Bandwidth Products) controlled by electro-optic modulators (350-80, Conoptics) were combined by a polarizing beamsplitting cube (Thorlabs) to excite the synthetic dyes (810 nm) and ChR2-tdimer2 (1056 nm) simultaneously. To combine the blue light used for stimulation with the IR lasers, we used a 470/40 bandpass and a 725DCXR dichoic mirror (Chroma).

1. Kugler, S. et al. Neuron-specific expression of therapeutic proteins: evaluation of different cellular promoters in recombinant adenoviral vectors. *Mol Cell Neurosci* **17**, 78-96 (2001).
2. Stoppini, L., Buchs, P.A. & Muller, D. A simple method for organotypic cultures of nervous tissue. *Journal of Neuroscience Methods* **37**, 173-82 (1991).
3. Pologruto, T.A., Sabatini, B.L. & Svoboda, K. ScanImage: Flexible software for operating laser scanning microscopes. *Biomed Eng Online* **2**, 13 (2003).